

EFFECT OF CeO_2 DOPING ON THE STRUCTURE, ELECTRICAL CONDUCTIVITY AND ETHANOL GAS SENSING PROPERTIES OF NANOCRYSTALLINE ZnO SENSORS

A. M. El-Sayed [1,*], F. M. Ismail [1], M. H. Khder [2], M. E. M. Hassouna [2] and S. M. Yakout [1]

[1] Inorganic Chemistry Department, National Research Centre, Tahrir Street, Dokki, 12622 Cairo, Egypt

[2] Department of Chemistry, Faculty of Science, Beni-Sueif University, Egypt

*Correspondence Author: ahmed_elsayed_3@hotmail.com

Submitted: June 30, 2012 ***Accepted: Aug. 3, 2012*** ***Published: Sep. 1, 2012***

Abstract- Nanocrystalline sensors having the general formula ZnO + x wt% CeO_2, where x = 0, 2, 4 and 6 were prepared by chemical precipitation method and sintered at 400, 600 and 800 ^oC for 2h in static air atmosphere. The crystal structure and the morphology of the prepared samples were investigated and characterized by using XRD, IR, SEM and TEM techniques. The investigation revealed that the average crystallites size increases with increasing the sintering temperature. The electrical conductivity is found to increase with CeO_2 additions and sintering temperature. Gas sensing properties of the prepared samples were also investigated. The effect of CeO_2 content and sintering temperature on the structure, electrical conductivity and ethanol gas sensing properties of the prepared samples are discussed.

Index terms: ZnO nanoparticles, Ce-doping, ethanol gas sensor.

I. INTRODUCTION

Many industrial and commercial activities required the detection, quantification and controlling of ethanol gas concentration [1]. Ethanol gas sensors are extensively used for breath analyzer of drivers which aid to reduce the number of roads accidents, monitoring of fermentation, foodstuffs conserving and other processes in chemical industries [2-4]. In recent years, ZnO nanostructures have been studied as possible candidate for the fabrication of ethanol gas sensors due to their high surface area, low cost and high sensitivity [5-7]. The working principle of the ZnO as semiconductor gas sensors is based on the change in its resistance after exposure to ethanol gas. The reaction of ethanol gas with the chemisorbed oxygen ions species (O^-, O^{2-}) on the sensor surface is accompanied with liberate of electrons to the conduction band which leads to the observed change in resistance [7-8]. The sensing properties of the ZnO gas sensor can be improved by decreasing its particles size and consequently increasing the surface area which provides more surface active sites for gases to adsorb and interact [9]. The doping of ZnO with suitable dopant is an important and effective way to improve its sensing properties [10]. Many authors have attempted to improve the gas sensing properties of ZnO toward ethanol gas via using some additives such as noble metal Pd, Pt and Au [11-13], transition or main-group metal oxide including of TiO_2, CuO, CoO, and RuO_2 [14-17]. The effect of Al-, In-, Cu-, Fe and Sn-dopants on the response of a ZnO thin film gas sensor to ethanol vapour has been studied by Paraguay et al. [18]. Rare earth oxides are well known to display a high surface basicity, fast oxygen ion mobility and interesting catalytic properties which are very important in gas sensing [19]. The present work aims to prepare the pure and Ce-doped ZnO nanoparticles sintered at different temperature and to study the effect of CeO_2 content and sintering temperature on the structure, electrical conductivity and sensing properties toward ethanol gas of nanocrystalline ZnO.

II. EXPERIMENTAL METHODS

a- Synthesis of ZnO nanoparticles

Synthesis of zinc oxide nanoparticles was carried out by using a simple chemical precipitation method using high purity $Zn(CH_3COO)_2{\cdot}2H_2O$ (99.60%) and NH_4OH. The solution of zinc acetate dihydrate with the concentration of 0.2 mol/L was prepared. Diluted ammonium hydroxide was also prepared and added drop wise to the prepared zinc acetate dihydrate solution at room temperature with continuous stirring to yield precipitates of zinc hydroxide

at pH value of 8. The precipitates was aged for one hour, and then separated from the rest of the liquid by filtering and washed several times with deionized water, and followed by drying at 105 ^{o}C. The obtained powder was crushed and calcined in a muffle furnace at the temperature of 400 ^{o}C for 4 hours, then left to cool in atmospheric air to room temperature.

b- Sensors fabrication

Proper amounts of CeO_2 were added to the prepared ZnO powder with the ratio of 0, 2, 4 and 6 wt %. The obtained mixtures were ground in an agate mortar to get homogeneous and good mixing mixtures. The resulting mixtures were used to fabricate the sensor pellets of 12 mm in diameter and 2 mm thick by applying a pressure of 5 ton cm^3 using hydraulic press followed by sintering at 400, 600 and 800 ^{o}C for 2 h.

c- Characterization and measurement

The prepared samples were investigated by X-ray powder diffraction (XRD) using X-ray diffraction diffractometer (model-Bruker AXS D_8 advance) with copper radiation, infrared spectra (IR) using Nexus 670 FTIR spectrophotometer (Nicolet, USA), Scanning electron microscope (SEM) using SEM JEOL models, JXA-480A Electron Probe Micro analyzer and transmission electron microscope (TEM) using JEOL JEM-1230 operating at 120 KV attached to CCD camera. a. c. electrical conductivity as well as ethanol gas sensing properties of the different sensor samples were measured in the temperature range from 30 up to 410 ^{o}C using LCR meter (Hisester, model Hioki 3532, made in Japan) at frequency of 1 KHz and applied 5 V. The sample chamber is a closed glass cell contains the sensor sample surrounded by cylindrical ceramic furnace with controlled temperature device. The desired ethanol gas concentrations were obtained by injection a known volume of ethanol vapor using a micro-syringe through air tight rubber port into the glass chamber. The sensitivity (S) of the sensor samples were measured and calculated as the ratio of the electrical resistance in air atmosphere (R_{air}) to that in air plus ethanol gas (R_{gas}) in the temperature range from 30 up to 410 ^{o}C by using the following relation [20]:

$$S = R_{air} / R_{gas} \qquad (1)$$

III. RESULTS AND DISSCUSSION

a- The structure of the products

The X-ray diffraction investigation carried out on the prepared ZnO revealed that the obtained ZnO is pure single phase having hexagonal wurtzite structure with a good crystalline character according to the standard data (JCPDS, card file No. 36-1451). The average

crystallite size (D) of the prepared ZnO is approximately 34.5 nm as estimated from the full width at half maximum (FWHM) of the most intense peaks using Debye-Scherer equation which confirmed the formation of nanoparticles ZnO. The X-ray diffraction patterns of the pure and CeO_2-doped ZnO nanoparticles sintered at 400 and 800 ^oC are shown in Figure 1. All the diffraction peaks of the pure and CeO_2-doped ZnO samples could be indexed to hexagonal wurtzite structure for ZnO and to cubic structure for CeO_2 which consistent with the standard JCPDS (card file: No. 81-0792). Generally, there is no change in the position of the diffraction peaks with CeO_2 additions or sintering temperature and there is no evidence for interaction between the two components or the formation of a new complex oxide during the sintering temperatures. It is clear that with increasing CeO_2 content up to 6 wt %, the intensity of the characteristic CeO_2 peaks increased. The average crystallite size (D) of the pure and CeO_2-doped ZnO samples sintered at 400, 600 and 800 ^oC were estimated and tabulated in Table 1. It was found that the average crystallite size for the prepared samples increased with increasing the sintering temperature.

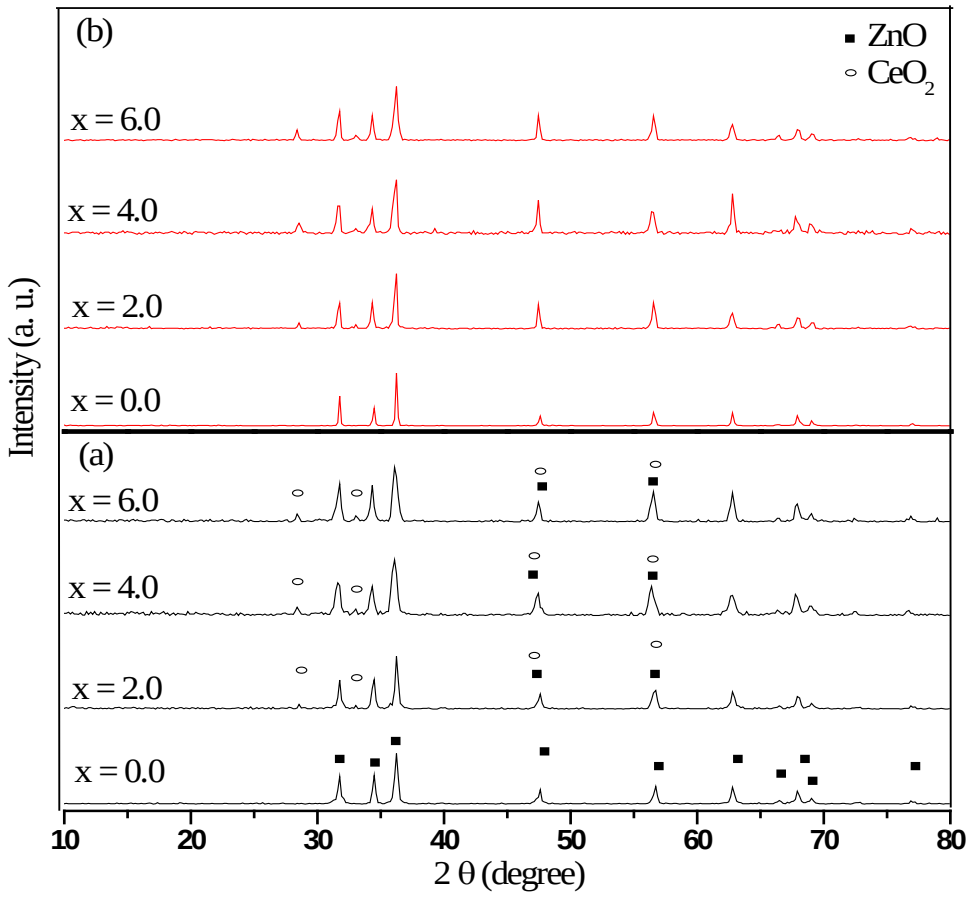


Figure 1. X-ray diffraction patterns of the prepared ZnO+ x wt% CeO_2 samples sintered at (a): 400 ^oC and (b): 800 ^oC.

Table 1: The obtained data of ZnO + x wt % CeO_2 samples sintered at different temperature.

x	400 °C				600 °C				800 °C			
	D (nm)	ν_1 (cm^{-1})	ΔE (eV)	S	D (nm)	ν_1 (cm^{-1})	ΔE (eV)	S	D (nm)	ν_1 (cm^{-1})	ΔE (eV)	S
0	55	437	0.8	19	92.4	437	0.86	12.4	181	419	1.04	7.1
2	47	442	0.77	59	78	423	0.82	42.3	93	431	0.94	28.5
4	44	453	0.74	71	72.5	452	0.8	55.1	88	434	0.89	35.9
6	40.5	500	0.91	41.1	68	497	1.1	31.5	83	461	1.27	22.1

b- IR investigation

Figure 2 shows the Infrared spectra of pure and CeO_2-doped ZnO nanoparticles samples sintered at 400 and 800 °C. It can be seen that, the characteristic absorption band for the prepared ZnO sample appeared at 461 cm^{-1}, which is attributed to stretching vibration of Zn-O bond [21]. This band slightly shifted to lower wavenumber and its shape became slightly more broadening with increasing the sintering temperature. This may be due to the increasing in the particles size or aggregation of the particles with increasing the sintering temperature [22]. The characteristic absorption band of the prepared ZnO overlapped with the CeO_2 absorption band which observed at ~ 433 cm^{-1} to give more broadening one (ν_1) for all doped samples as indicated in Table 1. It is also noticed that, the bands position for the doped samples slightly shifted to higher wavenumber with CeO_2 additions at the same sintering temperature. This may be due to the change in the particles size or the degree of aggregation by the addition of CeO_2.

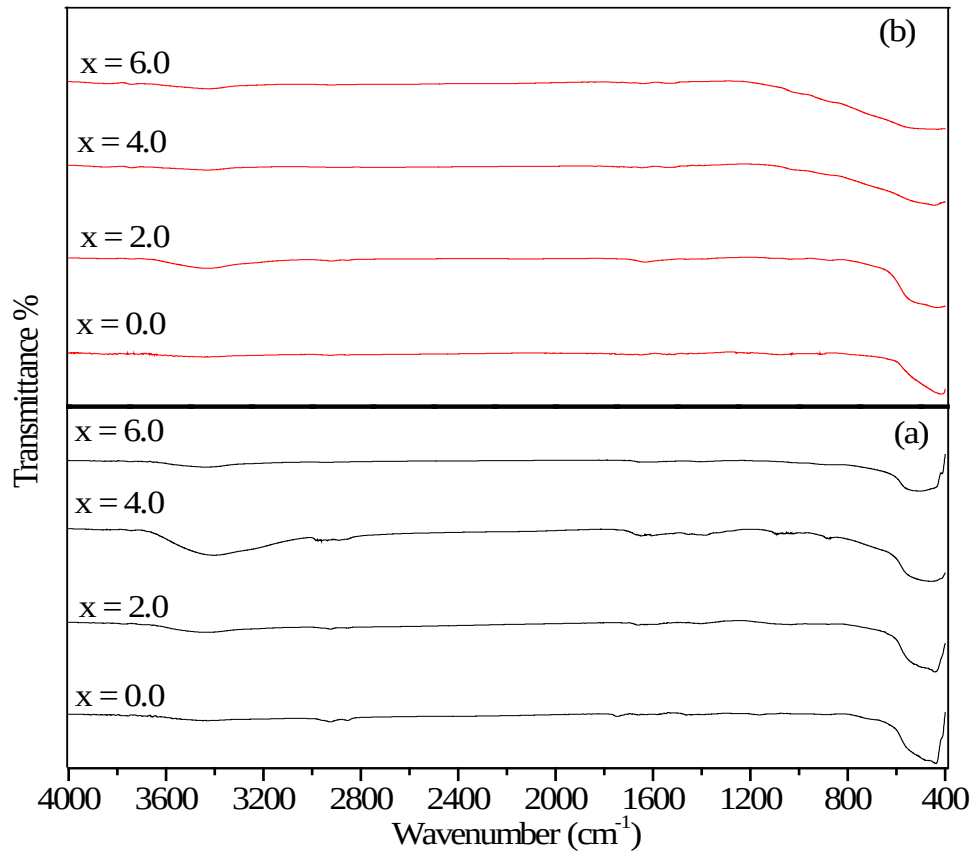


Figure 2. Infrared spectra of the prepared ZnO + x wt% CeO_2 samples sintered at (a): 400 ^oC and (b): 800 ^oC.

c- SEM analysis

The scanning electron microscope photographs of pure and CeO_2-doped ZnO samples sintered at 400 and 800 ^oC for 2 hours are shown in Figures 3 and 4 respectively. It can be seen that, the grains size of the pure ZnO and the volume of the pores which located at grain boundaries and that inside the grains tend to increase with sintering temperature. The average grain size of the pure ZnO tends to decrease by the increasing CeO_2 content which indicates that the addition of CeO_2 impedes ZnO grain growth. The observed large grains in the case of the pure sample sintered at 800 ^oC, Fig. 4 (a), presumably due the promotion of crystalline phase and neck growth between particles as the temperature increased [23]. The morphology of the doped samples sintered at 400 ^oC shows that it composed of nearly homogeneous spherical grains. Where, with increasing the sintering temperature up to 800 ^oC the grains became more uniform with larger grains size. The presence of ZnO grains having hexagonal shape beside the cubic grains of the added CeO_2 can be seen from the image of the sensor sample with x = 6 and sintered at 800 ^oC (Figure 4d).

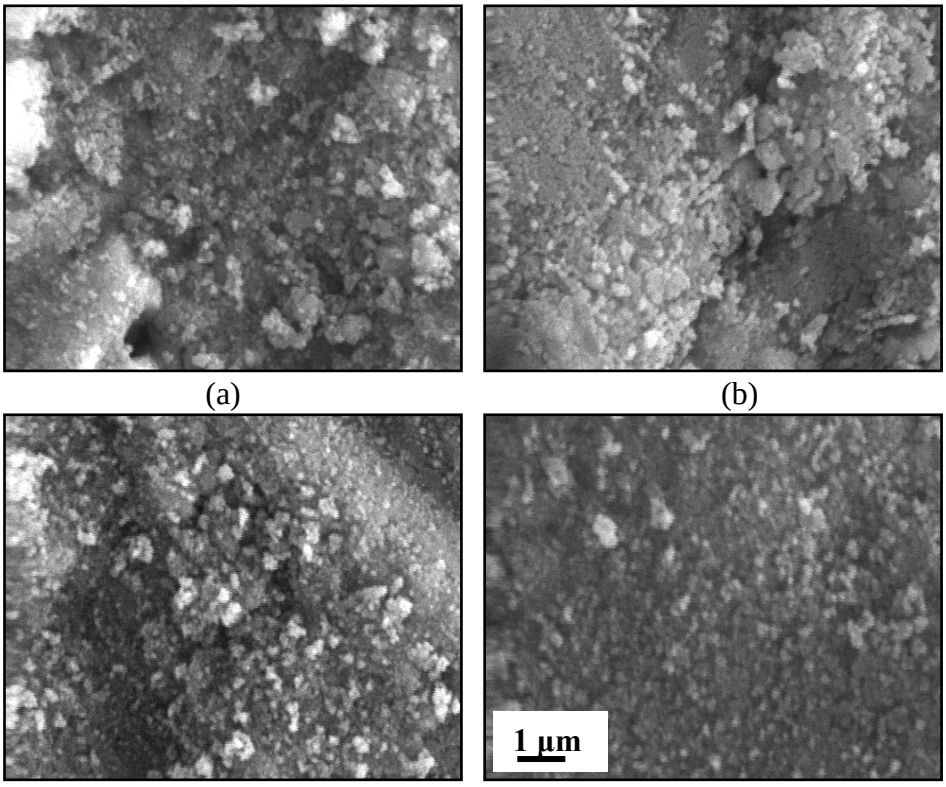


Figure 3. SEM photographs of ZnO + x wt% CeO_2 samples sintered at 400 ^oC, (a): x = 0, (b): x = 2, (c): x = 4 and (d): x = 6.

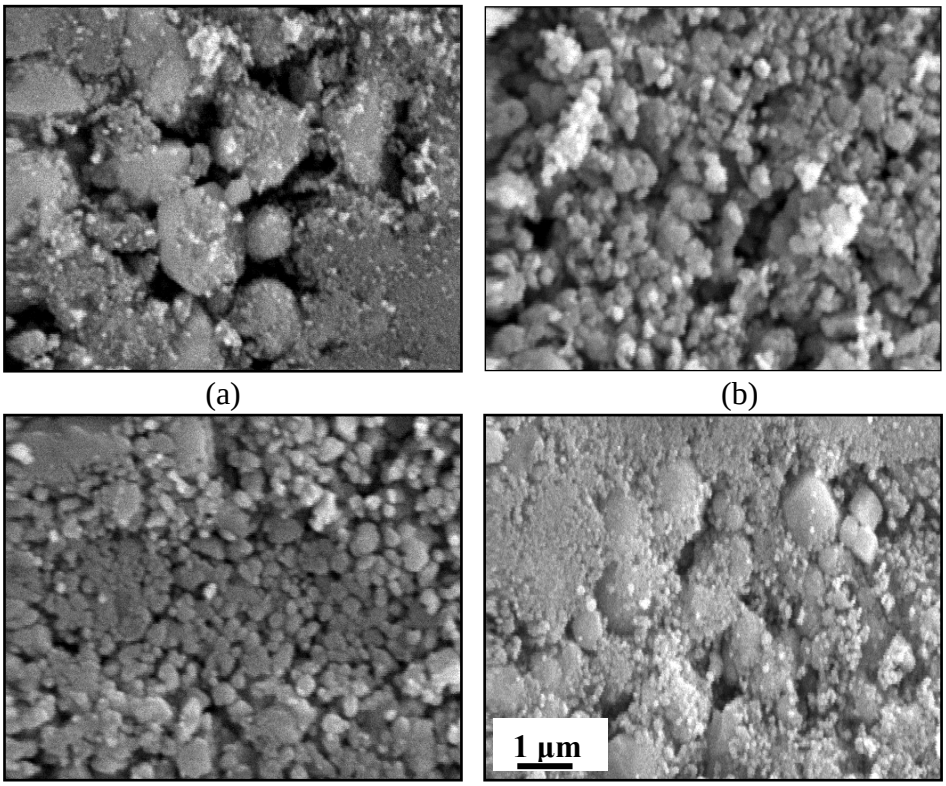


Figure 4. SEM photographs of ZnO + x wt% CeO_2 samples sintered at 800 ^oC, (a): x = 0, (b): x = 2, (c): x = 4 and (d): x = 6.

d- TEM analysis

Figures 5 and 6 depict the transmission electron microscope photographs of the pure and CeO_2-doped ZnO samples sintered at 400 and 800 ^oC respectively. It was found that, the photographs of the pure ZnO nanoparticles sintered at 400 ^oC, Fig. 5 (a), shows some agglomeration and the particles have a hexagonal shape with the average particle size of 60 nm. With increasing the sintering temperature the average particle size increased (Fig. 6a). While, the average particle size decreases with CeO_2 additions at the same sintering temperature (Figs. 5 and 6). These results show that CeO_2 doping material may be act as inhibitor which resists the ZnO grain growth during the sintering temperature and the hexagonal shape of the ZnO nanoparticles is clearly enhanced by the addition of CeO_2.

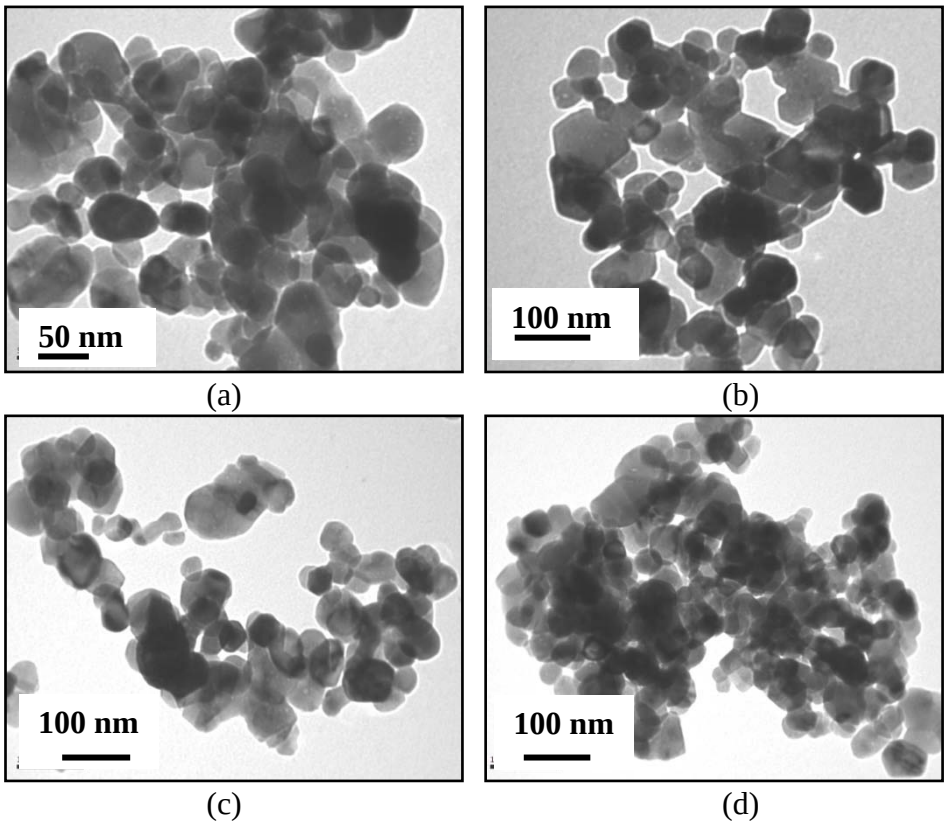


Figure 5. TEM photographs of ZnO + x wt% CeO_2 samples sintered at 400 ^oC, (a): x = 0, (b): x = 2, (c): x = 4 and (d): x = 6.

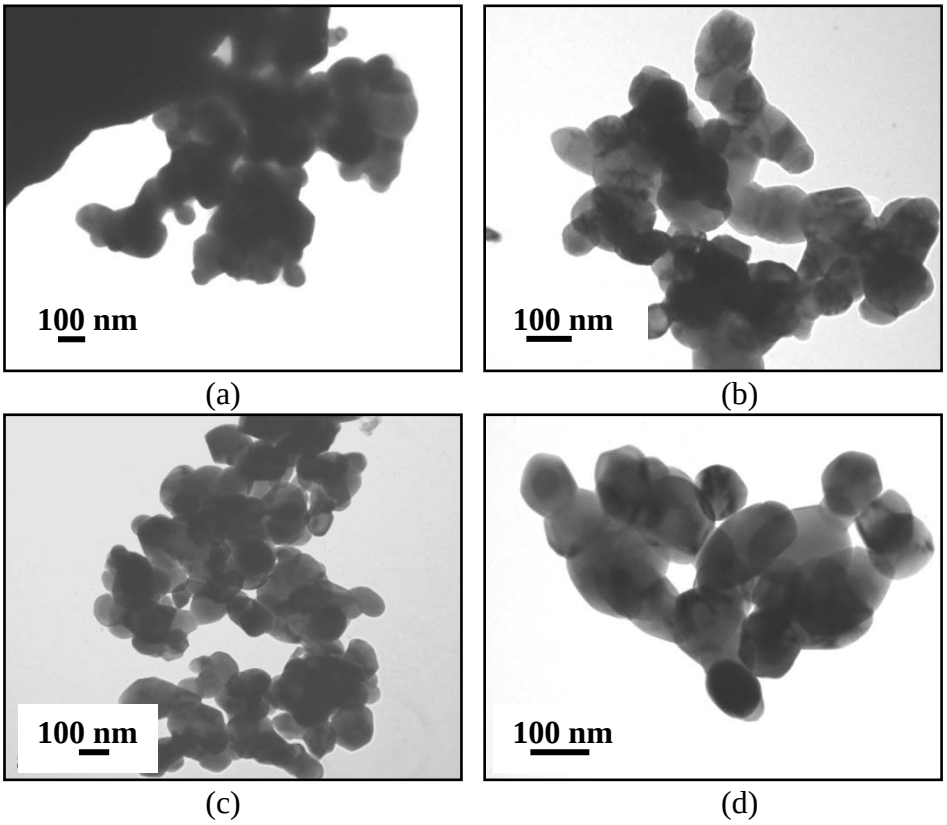


Figure 6. TEM photographs of ZnO + x wt% CeO_2 samples sintered at 800 ^oC, (a): x = 0, (b): x = 2, (c): x = 4 and (d): x = 6.

e- Electrical conductivity measurements

The variation of the electrical conductivity with temperature for pure and CeO_2-doped ZnO samples sintered at 400 and 800 ^oC are shown in Figure 7. Generally, the features of the curves are nearly the same. Each curve consists of three different temperature regions denoted as AB, BC and CD. At low temperature regions (AB), the electrical conductivity of the samples slightly increases with increasing the temperature which may be attributed to the thermal excitation of impurity electrons presumably present. The decreases in the electrical conductivity in BC regions are likely to be in relation with the adsorbed of oxygen species on the surfaces of the ZnO nanoparticles [24]. The adsorbed oxygen molecules turning into oxygen ions ($O_2^- \rightarrow 2O^- \rightarrow O^{2-}$) by accepting free electrons from the ZnO conduction band which leads to the increase in the resistance and consequently the decreasing in the electrical conductivity. With increasing the temperature, the intrinsic behaviour is dominant and the electrical conductivity in the CD regions was found to increases again, probably due to the thermal excitation of electrons and the desorption of oxygen species [24].

The electrical conductivity of the pure and CeO_2-doped ZnO samples is found to increase with increasing the sintering temperature from 400 up to 800 ^oC as shown in Figure 7 (a and

b). This may be attributed to the increase in the charge carriers concentration due to the increase of oxygen vacancies by increasing the sintering temperature [25]. With increasing the sintering temperature, the boundaries of the grains get diffused which resulting in the increasing of the grains size which cause the electrical conductivity to increase [26]. With CeO_2 additions the electrical conductivity of the different samples sintered temperature was found to increase. This may be due to the increase of the charge carriers' concentration, which results in the decrease of the resistance of ZnO samples [27]. The intrinsic activation energy (ΔE) of the measured samples at higher temperature region was calculated and presented in Table 1.

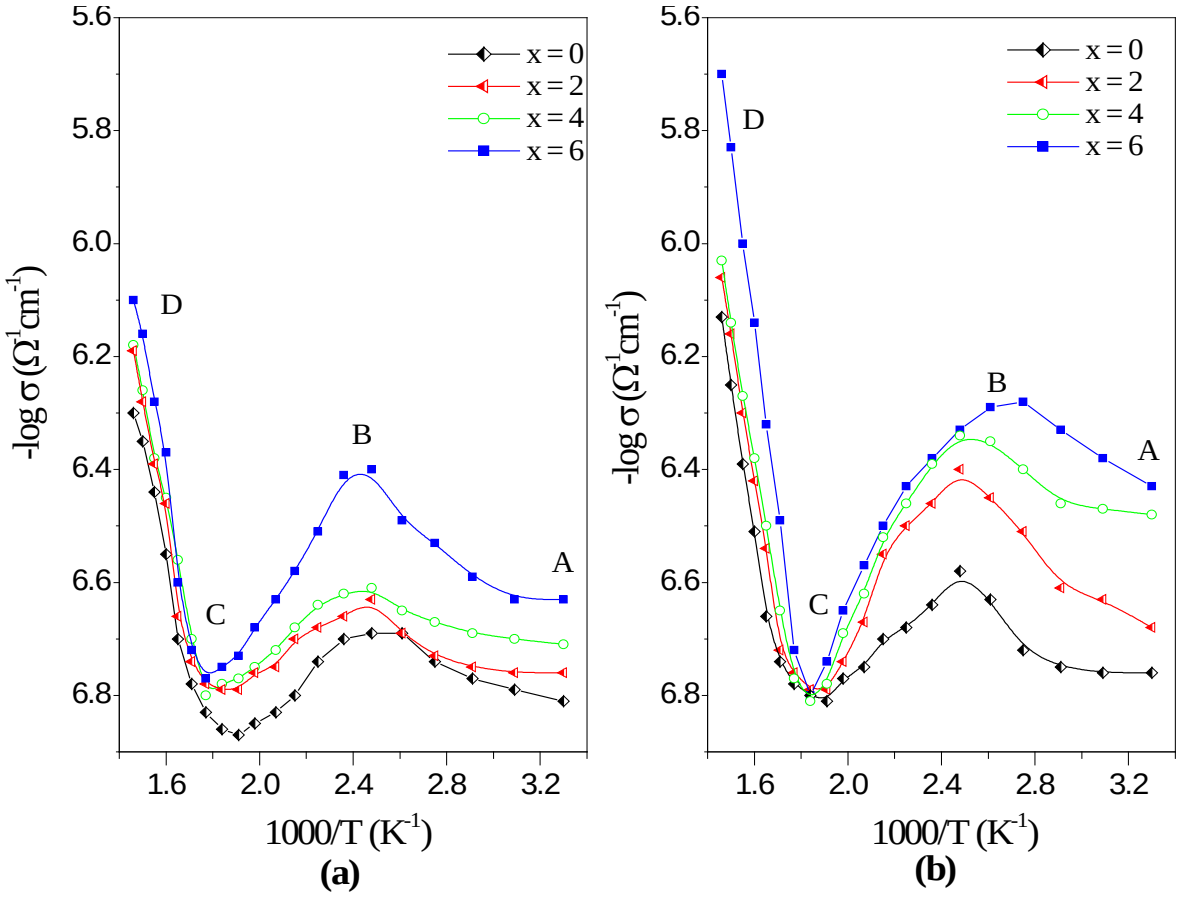


Figure 7. The variation of the electrical conductivity with temperature for ZnO + x wt% CeO_2 samples sintered at (a): 400 ^oC and (b): 800 ^oC.

f- Gas sensing properties

Figure 8 depicts the variation of the sensitivity with temperature for pure and CeO_2-doped ZnO sensor samples sintered at 400, 600 and 800 ^oC toward 100 ppm ethanol gas. It can be seen that, the sensitivity gradually increases with increasing the temperature and reached its maximum value at 310 ^oC (operating temperature) for all the measured samples. With

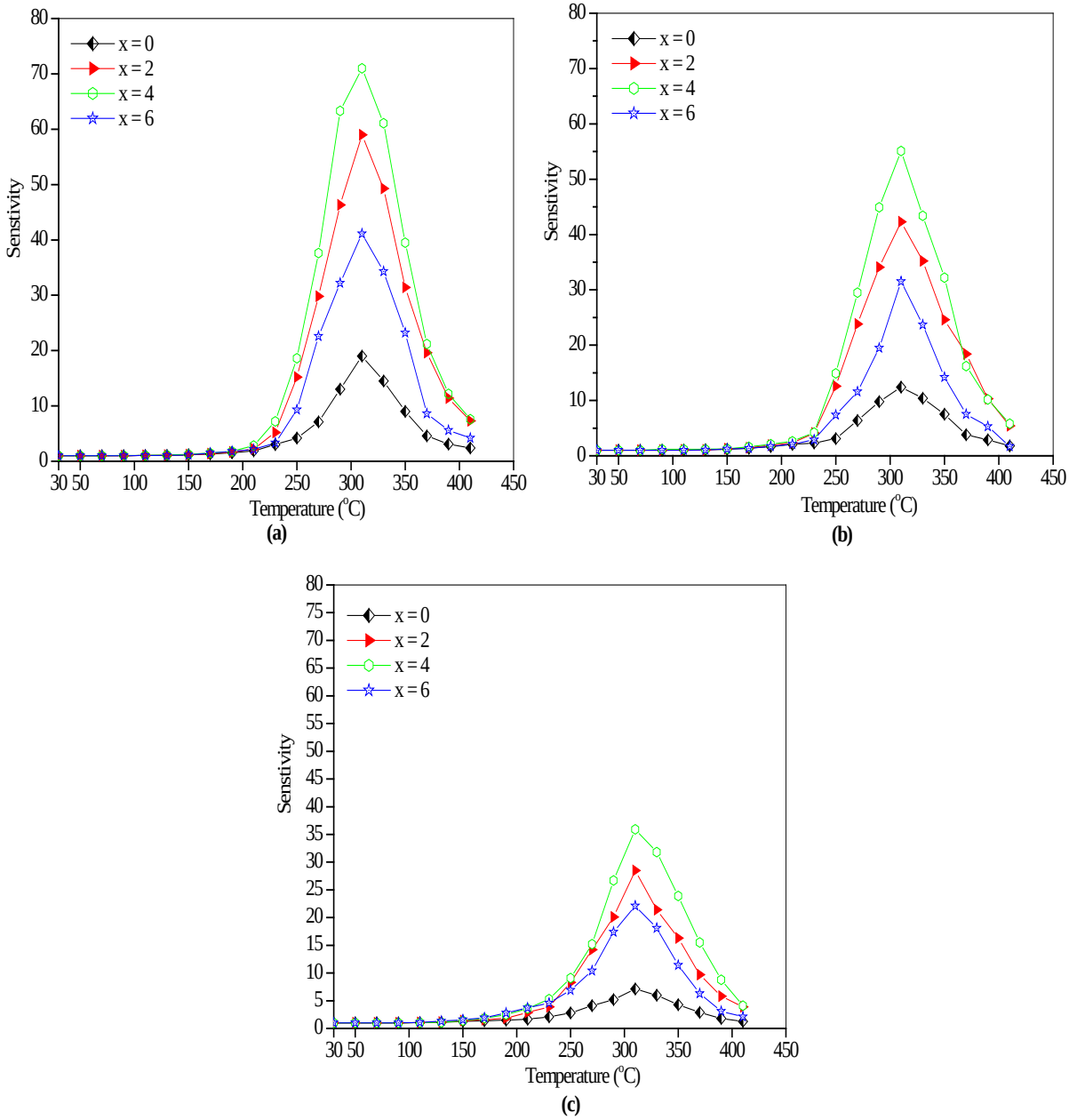


Figure 8. The variation of the sensitivity with temperature toward 100 ppm ethanol gas for ZnO + x wt % CeO_2 sensor samples sintered at (a): 400, (b): 600 and (c): 800 °C.

increasing the temperature above 310 °C, the sensitivity of the sensor samples decreases. The change in the sensitivity with temperature depends on the interaction between the adsorbed oxygen species and ethanol gas [5, 7]. When the pure and CeO_2-doped ZnO sensor samples heated, oxygen molecules begin to adsorb and dissociate ($O_2^- \rightarrow 2O^- \rightarrow O^{2-}$) on their surfaces and its concentration rise gradually with increasing the temperature until certain temperature which accompanied with the increase in the electrical resistance. While, at higher temperature desorption of the oxygen species from the sensor surfaces leads to the decrease in the oxygen

species concentration. So, the high sensitivity values to ethanol gas at the temperature of 310 ^{o}C can be attributed to the high concentration of adsorbed oxygen species and high oxidation activity of ethanol gas according to the following equations [10, 28 and 29]:

$$C_2H_5OH + 6O^{-} (ads) \longrightarrow 2CO_2 + 3H_2O + 6e \quad (2)$$

or

$$C_2H_5OH + 6O^{2-} (ads) \longrightarrow 2CO_2 + 3H_2O + 12e \quad (3)$$

The sensitivity of the sensor samples was found to decrease with increasing the sintering temperature from 400 up to 800 ^{o}C, Fig 8. The decreasing in the sensitivity with increasing the sintering temperature may be due to the effect of the particle size, where the smaller particles size having high surface area with more active sites of the gas sensor is believed to be one of the most important parameters that responsible for enhancing the sensing properties [6]. With increasing the sintering temperature up to 800 ^{o}C, the average particle size of the sensor samples increase and consequently the surface area decrease which provide less active sites for adsorption and interaction between the adsorbed oxygen species and ethanol gas which lead to the decrease in sensitivity.

The variation of the sensitivity with different CeO_2 concentration for ZnO + x wt% CeO_2 sensor samples sintered at different temperature is shown in Figure 9. It can be seen that, the sensitivity of the sensors increases with increasing CeO_2 concentration up to 4 wt% and then decreases with further CeO_2 additions at different sintering temperature. The CeO_2 additions to ZnO sensors up to 4 wt% can promote the ethanol dehydrogenation reaction in the form of catalysts and improve ZnO surface basicity which enhances the sensitivity towards ethanol gas [30]. On the other hand, the increasing in CeO_2 doping concentration to 6 wt % may be cause a high covering of ZnO surface which reducing the available adsorption sites on ZnO surface and leads to the observed decrease in the sensitivity. Therefore, appropriate CeO_2 doping concentration seems to be benefit to improve the gas sensing properties.

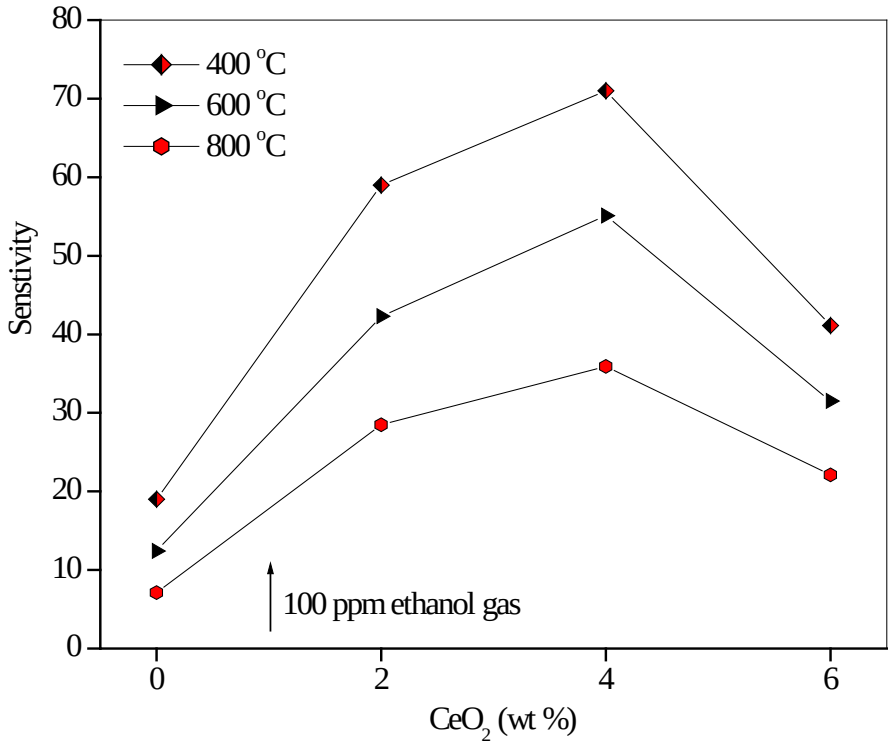


Figure 9. The variation of the sensitivity with CeO_2 concentration for ZnO + x wt % CeO_2 sensor samples sintered at different temperature, operating temperature 310 ^oC.

Figure 10 shows the variation of sensitivity with ethanol gas concentration for pure and CeO_2-doped ZnO sensor samples sintered at 400 ^oC, operating temperature 310 ^oC. With respect to the undoped ZnO sample, the sensitivity linearly increases with increasing the concentration of ethanol gas up to 200 ppm. While, above 200 ppm, the sensitivity slowly increased. On the other hand, CeO_2-doped ZnO sensors samples show nearly linear increases of sensitivity up to 400 ppm then after the sensitivity slowly increased with increasing the concentration up to 2000 ppm. The sensor sample containing 4 wt% CeO_2 revealed the higher sensitivity values than that of the other sensor samples which implies that it is candidate for using in the applications that require the detection of lower and higher ethanol gas concentrations with high sensitivity.

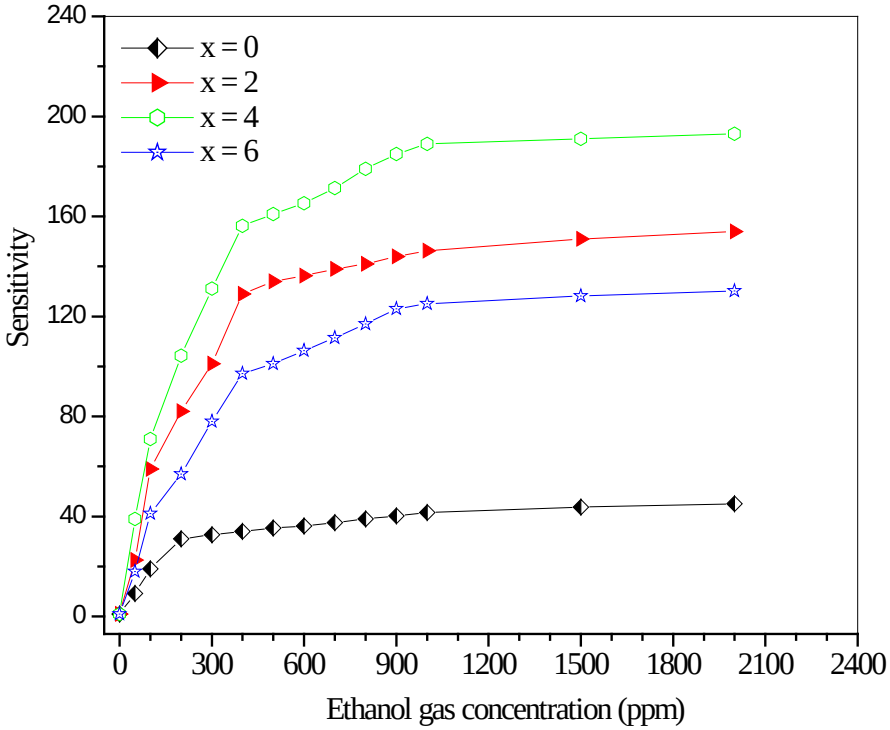


Figure 10. The variation of sensitivity with ethanol gas concentration for ZnO + x wt % CeO_2 sensor samples sintered at 400 ^oC, operating temperature 310 ^oC.

The response time is usually defined as the time taken to achieve at least 90 % of the final change in resistance during gas exposure. While, the recovery time is generally defined as the time taken for the sensor to get back at least 90 % of its original value when re-exposed to air ambient by maintaining the operating temperature constant [31]. Figure 11 depicts the variation of the sensitivity with time (seconds) for pure ZnO and ZnO containing 4 wt% CeO_2 sensor samples sintered at 400 ^oC during exposure to 100 ppm ethanol gas and re-exposure to air respectively. The response times for the pure ZnO and ZnO containing 4 wt% CeO_2 sensor samples, Figure 11a, were found to be 15 and 12 second respectively. While, the recovery times for these sensor samples, Figure 11b, were 12 and 10 second respectively. Among the investigated pure and doped sensor samples, it was found that the ZnO containing 4 wt% CeO_2 sensor sample sintered at 400 ^oC is the more suitable sample to be used as ethanol gas sensor at different ethanol gas concentration with high sensitivity values and rapid response time and short recovery time.

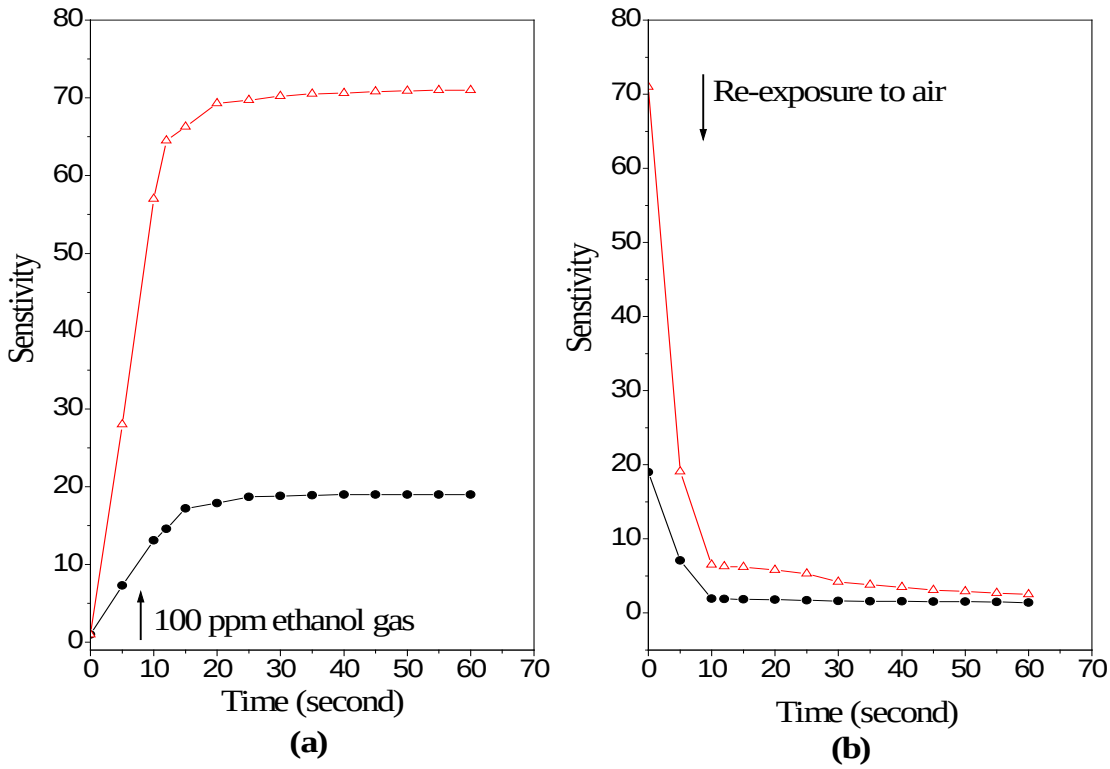


Figure 11. The variation of the sensitivity with time (seconds) for undoped ZnO (●) and ZnO containing 4 wt% CeO_2 (Δ) sensor samples sintered at 400 ^oC during (a) exposure to 100 ppm ethanol gas and (b) re-exposure to air, operating temperature 310 ^oC.

IV. CONCLUSIONS

ZnO nanoparticles were synthesized by chemical precipitation method. XRD, IR, SEM and TEM investigations confirmed the formation of ZnO having wurtzite hexagonal structure and the average particle size of the prepared ZnO sensors increased with increasing the sintering temperature and decreased with CeO_2 additions. The electrical conductivity was found to increase with the CeO_2 additions and sintering temperature. The sensitivity was found to decrease with sintering temperature and effects with CeO_2 content. The obtained data indicated that ZnO containing 4 wt% CeO_2 sensor sample sintered at 400 ^oC has a higher sensitivity values toward ethanol gas with rapid response and short recovery time.

REFERENCES

[1] J. Shi, J. Li, Y. Zhu, F. Wei and X. Zhang, Nanosized $SrCO_3$-based chemiluminescence sensor for ethanol, Analytica Chimica Acta, Vol. 466, 2002, pp. 69-78.

[2] G. Neri, A. Bonavita, G. Micali, N. Donato, F. A. Deorsola, P. Mossino, I. Amato and B. De Benedetti, Ethanol sensors based on Pt-doped tin oxide nanopowders synthesised by gel-combustion, Sensors and Actuators B, Vol. 117, 2006, pp. 196-204.

[3] B. P. J. de Lacy Costello, R. J . Ewen, N. Guernion and N. M. Ratcliffe, Highly sensitive mixed oxide sensors for the detection of ethanol, Sensors and Actuators B, Vol. 87, 2002, pp. 207-210.

[4] N. V. Hieu, N. A. P. Duc, T. Trung, M. A. Tuan and N. D. Chien, Gas-sensing properties of tin oxide doped with metal oxides and carbon nanotubes: A competitive sensor for ethanol and liquid petroleum gas, Sensors and Actuators B: Chemical, Vol. 144, 2010, pp. 450-456.

[5] S. D. Shinde, G. E. Patil, D. D. Kajale, D. V. Ahire, V. B. Gaikwad and G. H. Jain, Synthesis of ZnO nanorods by hydrothermal method for gas sensing applications, International Journal on Smart Sensing and Intelligent Systems, Vol. 5, No. 1, 2012, pp. 57-70.

[6] R. C. Singh, O. Singh, M. P. Singh and P. S. Chandi, Synthesis of zinc oxide nanorods and nanoparticles by chemical route and their comparative study as ethanol sensors, Sensors and Actuators B, Vol. 135, 2008, pp. 352-357.

[7] L. Wang, Y. Kang, X. Liu, S. Zhang, W. Huang and S. Wang, ZnO nanorod gas sensor for ethanol detection, Sensors and Actuators B, Vol. 162, 2012, pp. 237- 243.

[8] K. Wetchakun, T. Samerjai, N. Tamaekong, C. Liewhiran, C. Siriwong, V. Kruefu, A. Wisitsoraat, A. Tuantranont and S. Phanichphant, Semiconducting metal oxides as sensors for environmentally hazardous gases, Sensors and Actuators B, Vol. 160, 2011, pp. 580-591.

[9] S. Choopun, N. Hongsith, P. Mangkorntong and N. Mangkorntong, Zinc oxide nanobelts by RF sputtering for ethanol sensor, Physica E, Vol. 39, 2007, pp. 53-56.

[10] C. Ge, C. Xie, M. Hu, Y. Gui, Z. Bai and D. Zeng, Structural characteristics and UV-light enhanced gas sensitivity of La-doped ZnO nanoparticles, Materials Science and Engineering B, Vol. 141, 2007, pp. 43-48.

[11] C. Liewhiran and S. Phanichphant, Effects of Palladium Loading on the Response of a Thick Film Flame-made ZnO Gas Sensor for Detection of Ethanol Vapor, Sensors, Vol. 7, 2007, pp. 1159-1184.

[12] N. Hongsith and S. Choopun, Effect of Platinum Impregnation on ZnO Tetrapods for Ethanol Sensor, Advanced Materials Research, Vol. 55-57, 2008, pp. 289-292.

[13] E. Wongrat, P. Pimpang and S. Choopun, Comparative study of ethanol sensor based on gold nanoparticles: ZnO nanostructure and gold: ZnO nanostructure, Applied Surface Science, Vol. 256, 2009, pp. 968-971.

[14] K. Zheng, L. Gu, D. Sun, X. Mo and G. Chen, The properties of ethanol gas sensor based on Ti doped ZnO nanotetrapods, Materials Science and Engineering B, Vol. 166, 2010, pp. 104-107.

[15] L. Peng, T.-F. Xie, M. Yang, P. Wang, D. Xu, S. Pang and D.-J. Wang, Light induced enhancing gas sensitivity of copper-doped zinc oxide at room temperature, Sensors and Actuators B, Vol. 131, 2008, pp. 660-664.

[16] Y.-J. Li, K.-M. Li, C.-Y. Wang, C.-I. Kuo and L.-J. Chen, Low-temperature electrodeposited Co-doped ZnO nanorods with enhanced ethanol and CO sensing properties, Sensors and Actuators B, Vol. 161, 2012, pp. 734-739.

[17] S. C. Navale, V. Ravi and I. S. Mulla, Investigations on Ru doped ZnO: Strain calculations and gas sensing study, Sensors and Actuators B, Vol. 139, 2009, 466-470.

[18] F. D. Paraguay, M. Miki-Yoshida, J. Morales, J. Solis and W. L. Estrada, Influence of Al, In, Cu, Fe and Sn dopants on the response of thin film ZnO gas sensor to ethanol vapour, Thin Solid Films, Vol. 373, 2000, pp. 137-140.

[19] S. C. Tsang and C. Bulpitt, Rare earth oxide sensors for ethanol analysis, Sensors and Actuators B, Vol. 52, 1998, pp. 226-235.

[20] D. Haridas, A. Chowdhuri, K. Sreenivas and Vinay Gupta, Enhanced LPG response characteristics of SnO_2 thin film based sensors loaded with Pt clusters International journal on smart sensing and intelligent systems, Vol. 2, No. 3, 2009, pp. 503-514.

[21] S. Maensiri, P. Laokul and V. Promarak, Synthesis and optical properties of nanocrystalline ZnO powders by a simple method using zinc acetate dihydrate and poly(vinyl pyrrolidone), Journal of Crystal Growth, Vol. 289, 2006, pp. 102-106.

[22] C. P. Rezende, J. B. da Silva and N. D. S. Mohallem, Influence of drying on the characteristics of zinc oxide nanoparticles, Brazilian Journal of Physics, Vol. 39, 2009, pp. 248-251.

[23] Y. J. Kwon, K. H. Kim, C. S. Lim and K. B. Shim, Characterization of ZnO nanopowders synthesized by the polymerized complex method via an organochemical route, Journal of Ceramic Processing Research., Vol. 3, 2002, pp. 146-149.

[24] P. P. Sahaya and R. K. Nath, Al-doped ZnO thin films as methanol sensors, Sensors and Actuators B, Vol. 134, 2008, pp. 654-659.

[25] A. Sedky, T. A. El-Brolossy and S. B. Mohamed, Correlation between sintering temperature and properties of ZnO ceramic varistors, Journal of Physics and Chemistry of Solids, Vol. 73, , 2012, pp. 505-510.

[26] A. Singh, Synthesis, characterization, electrical and sensing properties of ZnO nanoparticles, Advanced Powder Technology, Vol. 21, 2010, pp. 609-613.

[27] D. Fangli, W. Ning, Z. Dongmei and S. Yingzhong, Preparation, characterization and infrared emissivity study of Ce-doped ZnO films, journal of rare earths, Vol. 28, No. 3, 2010, pp. 391-395.

[28] C. G. Dighavkar, A. V. Patil, S. J. Patil and R. Y. Borse, Effect on Ethanol Gas Sensing Performance of Cu Addition to TiO_2 Thick Films, Sensors & Transducers Journal, Vol. 116, 2010, pp. 28-37.

[29] N. K. Pawar, D. D. Kajale, G. E. Patil, V. G. Wagh, V. B. Gaikwad, M. K. Deore and G. H. Jain, nanostructured Fe_2O_3 thick film as an ethanol sensor, International Journal on Smart Sensing and Intelligent Systems, Vol. 5, NO. 2, June 2012, pp. 441-457.

[30] S. Matsushima, T. Maekawa, J. Tamaki, N. Miura and N. Yamazoe, Role of additives on alcohol sensing by semiconductor gas sensor, Chem. Lett., Vol. 18, 1989, pp. 845-848.

[31] M. Parmar and K. Rajanna, Copper (II) oxide thin film for methanol and ethanol sensing, International Journal on Smart Sensing and Intelligent Systems, Vol. 4, No. 4, 2011, pp. 710-725.